A-type potassium channel clusters revealed using a new statistical analysis of loose patch data

Samuel S.-H. Wang* and Stuart Thompson
*Neurosciences Program, and Department of Biological Sciences, Hopkins Marine Station, Stanford University, Pacific Grove, California 93950 USA

ABSTRACT The spatial distribution of ion channels over the surface of a neuron is an important determinant of its excitable properties. We introduce two measures of channel clustering for use in patch-clamp experiments: a normalized chi-squared statistic (η) and the number of zero-channel patches in a data set (Z). These statistics were calculated for data sets describing the distribution of A-type potassium channels on neurons of the nudibranch *Doriopsilla* and measurements of Ca-dependent outward current channels on bullfrog hair cells, as well as simulated channel distributions. When channels are clustered, η is approximately equal to the amount of current in a cluster. The analysis shows that somatic A-channels in the nudibranch are distributed in clusters of ~50 channels each. The clusters are <2 μm wide and are separated, on average, by 3.2 μm. Outward current channels on hair cells occur in clusters of ~27 channels each, in agreement with the original analysis. Channel clustering may reflect properties of the insertion or regulation of channels in the membrane.

INTRODUCTION

Mature neurons express a number of different voltage dependent ion channels; the spatial distribution of different channels in particular regions of the cell is an important determinant of neuronal function. Considerable evidence has accumulated showing that ion channels in mature neurons are not randomly distributed but tend to occur in higher densities at specific locations (Almers and Stirling, 1984; Poo, 1985; Thompson and Coombs, 1988; Premack et al., 1989). Good examples include the clustering of Na channels at the site of spike initiation (Catterall, 1981; Ellisman and Levinson, 1982) and the distribution of Ca channels, which are found in dendrites and presynaptic terminals but are scarce in axons (Katz and Miledi, 1969; Llinas and Nicholson, 1971).

When patch-clamp techniques are used to record ion channel activity on a fine spatial scale, one often observes a high degree of heterogeneity in channel number. Some membrane patches contain no channels, whereas other nearby patches on the same neuron contain numerous channels. This suggests that channel proteins tend to occur in clusters rather than being distributed randomly over the neuronal surface. A rule is emerging that ion channel proteins in mature cells are distributed in stable, nonuniform patterns and their lateral mobility is quite limited (Almers et al., 1982; Stuhmer and Almers, 1982; Beam et al., 1985; Angelides, 1986). Channel clustering has implications for the mechanisms involved in the targeting of ion channels to specific membrane regions and anchoring them in place. Moreover, clustering of channels and their anchoring to skeletal elements can influence channel function and excitability (Brehm et al., 1983; Young and Poo, 1983; Roberts et al., 1990).

There is a need to develop suitable statistical methods for evaluating the extent of channel clustering using patch-clamp data. We introduce two simple statistics that can be applied to this problem and illustrate their application to patch-clamp data sets from the literature. The experimental design that is most appropriate for using these statistics is described.

Address correspondence to S. Wang.

MATERIALS AND METHODS

The statistical treatment is applied to two experimental data sets. The spatial distribution of transient potassium current, I_A, on neuron cell bodies of the nudibranch *Doriopsilla* was measured using a loose patch method (Premack et al., 1989). These data include examples in which multiple patches were made on a single neuron, including one experiment where 31 patches were made (see Fig. 3). Whole-cell current was measured concurrently with the patch measurements. Single-channel current was determined by gigaseal patch. Roberts et al. (1990) provided a second data set that is appropriate for analysis and described the spatial distribution of Ca-dependent outward current channels in the basolateral region of vertebrate hair cells. The experimental methods are detailed elsewhere (Johnson and Thompson, 1989; Premack et al., 1989; Roberts et al., 1990).

These data sets include the following measurements to make them appropriate for the present analysis: (*a*) currents and accurate, unstretched patch areas; (*b*) the time and voltage dependence of opening probability so one can scale the patch data; and (*c*) the mean current density in the whole cell, either from whole cell clamp or from averaging a number of patches on a single cell. In addition, knowledge of the single channel current allows conclusions on the nature of current distributions to be converted to units of channels.

THEORY

Our two statistics for evaluating ion channel clustering are a normalized chi-squared statistic (η) and the number of patches in the data set that contain zero channels (Z). We determine the expectation and variance of these statistics for hypothetical models of the spatial distribution of ion channels. The square root of the variance is used to define the confidence interval for both statistics. We also give an approximation that allows the use of standard chi-squared tables for evaluation of confidence. These calculations allow us to test experimental data derived from patch-clamp experiments against specific models for channel distribution by computing η and Z

0006-3495/92/10/1018/08 $2.00

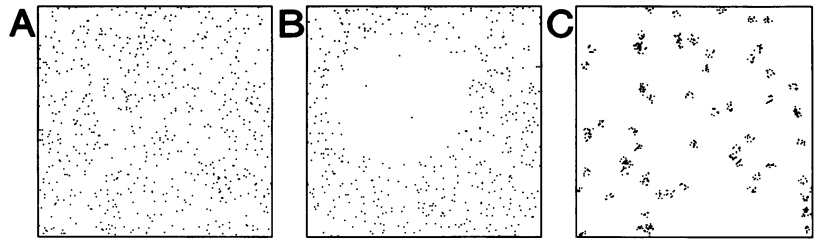

FIGURE 1 Various models of channel distributions. Examples for all models are for the same channel density, 0.26 channel/μm^2. (*A*) Randomly distributed channels. (*B*) A mosaic of two channel densities (see model 1, text). The membrane is divided into zones of area p and q with channel densities d_1 and d_2, respectively. (*C*) Randomly distributed clusters of channels (model 2). The clusters shown contain an average of 10 channels each in a Poisson distribution and are 2 μm in diameter. *C* is the best fit to the A-current loose patch data shown in Fig. 3. Boxes are 50 μm on a side.

for the data sets and comparing them to the expected values derived from the models.

A normalized chi-squared statistic

We call the ion channels on the surface of a cell "randomly distributed" if the expected channel density is the same everywhere and if there are no mechanisms to cluster or disperse channels. If membrane patches of constant area are sampled from randomly distributed channels, then x_i, the number of channels observed in a set of patches, will follow a Poisson distribution. One can test the hypothesis that channels are randomly distributed (Fig. 1 *A*) by calculating the ratio of the variance to the mean channel number. For a Poisson distribution, the variance-to-mean ratio is 1. Values >1 indicate clustering of channels, whereas values <1 indicate a more dispersed channel distribution than a random placement process would yield.

When membrane patches in the data set vary in area, as they normally do in patch-clamp experiments, this statistic must be modified to reflect the fact that each patch has its own expected number of channels. Customarily, investigators normalize current measurements by membrane area and report the results in units of current density. However, the variance of the current density is a function not only of the channel distribution but also of the distribution of patch areas and so is not a direct measure of channel clustering.

An appropriate modification of the variance-to-mean ratio that corrects for variability in patch area takes the form

$$\eta = \frac{1}{N-k}\sum_{i=1}^{N}\frac{(x_i - e_i)^2}{e_i}, \qquad (1)$$

where x_i and e_i are the observed and expected amount of current in the ith of N patches. Eq. 1 is the definition of $\chi^2_{N-1}/(N-k)$. k is the reduction in number of degrees of freedom resulting from the calculation of the mean current density on that cell, d_i. If expected current density is calculated by averaging patches on a cell, k is equal to the number of cells. If current density is taken from independent whole-cell measurements, $k = 0$. e_i is calculated by using the relation $e_i = A_i d_i$, where A_i is membrane area and d_i is the mean current density for the cell from which the patch is taken. If x_i and e_i are to be expressed as multiples of the single-channel current (i_{single} = 1 channel), x_i can be calculated by dividing observed current by the single-channel current i_{single} to get x_i. The results of the analysis below are derived and expressed most simply in terms of these "natural units."

For a random distribution of channels on a cell, the expectation and variance of η are

$$\langle\eta\rangle = i_{single}, \quad \mathrm{Var}(\eta) = \frac{2}{N-1}i^2_{single} + o\left(\frac{1}{N^2\bar{x}}\right)i^2_{single}, \qquad (2)$$

where $o(1/N^2\bar{x})$ denotes terms of order $1/N^2\bar{x}$.* In this case, η is distributed as $1/(N-1)\,\chi^2_{N-1}$ (Cramér, 1945).

Analysis based on the number of patches containing zero channels

In a given set of N patch recordings, define Z = (number of patches with zero observed channels). Z is a sensitive indicator of channel clustering. For a random distribution of channels,

$$\langle Z\rangle = \sum_{i=1}^{N} e^{-A_i d_i/i_{single}},$$

$$\mathrm{Var}(Z) = \sum_{i=1}^{N}\left(e^{-A_i d_i/i_{single}} - e^{-2A_i d_i/i_{single}}\right). \qquad (3)$$

For random channel distributions and for the other distributions we consider here, Z follows approximately a binomial distribution and the second expression reduces to $\mathrm{Var}(Z) \approx \langle Z\rangle\cdot(1 - \langle Z\rangle/N)$. This greatly simplifies the calculation of the confidence interval.

Models of clustered channel distributions

If η and Z do not fall within the confidence intervals given by Eqs. 2 and 3, then the channels are not ran-

* Notation used in this paper: $o(f)$, terms of order f or lower; $\bar{x}$, average value of x; $\langle x\rangle$, expected value of x.

domly distributed in the membrane. The following models of nonrandom channel distributions make testable predictions for η and Z.

Model 1: variable channel density

In this model, an electrode descending on the cell encounters a local current density d that varies with position. This mosaic or quiltwork of different densities is called a Cox process (Diggle, 1983).

For a given d and patch area A, the expected η can be expressed as

$$K(d, A) = i_{\text{single}} + \frac{A(d - \bar{d})^2 + (d - \bar{d})}{\bar{d}}. \quad (4)$$

$K(d, A)$ can be used as a kernel for convolution with the probability distribution of d to calculate the expected η for any hypothetical Cox process.

If we make the very general assumption that the probability distribution of d is symmetrical around its mean, $\bar{d}$, a simple expected value for η results:

$$\langle \eta \rangle = i_{\text{single}} + A \frac{\text{Var}(d)}{\bar{d}}. \quad (5)$$

This simple result has the interesting interpretation that in a broad range of models of variable current density, η increases linearly with patch area A, with an intercept of $\eta = i_{\text{single}}$ for zero patch area.

For purposes of fitting the observed molluscan loose-patch data, we give the expected values of η and Z for one simple, specific model of variable channel density. In this model (Fig. 1 *B*), patches of membrane may have one of two current densities, d_1 and d_2, with probability p and q, respectively. The expected values for η and Z are

$$\langle \eta \rangle = i_{\text{single}} + A\bar{d} \frac{pd_1^2 + qd_2^2 - \bar{d}^2}{\bar{d}^2}; \quad (6a)$$

$$\langle Z \rangle = \sum_{i=1}^{N} (pe^{-d_1 A_i / i_{\text{single}}} + qe^{-d_2 A_i / i_{\text{single}}}). \quad (6b)$$

When $d_2 = 0$, this model takes its extreme form, in which a fraction q of the membrane has no channels. In this case, $\langle Z \rangle = Nq$ (for $dA \gg 1$). One can test whether this condition applies to a given data set by dropping zero-channel patches from the data set. Since all of the remaining patches sample only the channel-containing portion of the membrane, it is expected that $\eta = i_{\text{single}}$ for this edited data set.

Model 2: channel clusters

In this model (Figure 1 *C*), channels occur in multichannel clusters. The mean and variance of the number of channels in a patch follow the relations $\langle x \rangle = Mm$, $\text{Var}(x) = Mv + m^2V$ (Pielou, 1977), where M and V are the mean and variance of the number of clusters in a patch, and m and v are the mean and variance of the number of channels in a cluster. If clusters are positioned at random in the membrane, the number of clusters found in a patch will follow a Poisson distribution. In this case, $M = V$ and $\langle \eta \rangle = \text{Var}(x)\, i_{\text{single}}/\langle x \rangle = (m + v/m) i_{\text{single}}$.

This shows that the expected value of η depends only on the single-channel current i_{single} and the cluster parameters m and v. Furthermore, we have found that in most cluster models, the term v/m does not contribute significantly to $\langle \eta \rangle$. When the number of channels per cluster is constant, $v/m = 0$. If the number of channels in a cluster is uniformly distributed over the interval $[0.5m, 1.5m]$, then $v/m = m/12$. If the number of channels per cluster is itself Poisson-distributed, then $v/m = 1$. We conclude that under a wide range of models of individual cluster composition, m dominates expectations for $\langle \eta \rangle$ and $\langle \eta \rangle$ is approximately equal to the amount of current in a channel cluster.

If the number of channels in a cluster is Poisson-distributed with mean m, then the resulting Poisson-Poisson distribution has the following expected values for η and Z:

$$\langle \eta \rangle = (m + 1) i_{\text{single}},$$

$$\text{Var}(\eta) = \frac{2}{N - 1} [(m + 1) i_{\text{single}}]^2 + o\left(\frac{m^3}{N\bar{x}}\right) i_{\text{single}}^2; \quad (7a)$$

$$\langle Z \rangle = \sum_{i=1}^{N} \exp\left[-\frac{A_i d_i}{m i_{\text{single}}} (1 - e^{-m}) \right] \approx \sum_{i=1}^{N} e^{-A_i d_i / m i_{\text{single}}}. \quad (7b)$$

If N or x is >10, η is distributed approximately as $i_{\text{single}}(m + 1)\, \chi^2_{N-1}/(N - 1)$; this allows the use of standard tables of the χ^2 distribution to evaluate values of η in this model. The approximation in Eq. 7b is valid with $m \gg 1$ and is exact when the number of channels per cluster is constant ($v = 0$). $\langle Z \rangle$ is dependent on the particular distribution of patch areas and thus must be calculated from experimental measurements. Note that the exponent in Eq. 7b, $A_i d_i / m i_{\text{single}}$, is the number of clusters expected in patch i.

In patch-clamp experiments, it is not always possible to distinguish between patches containing few channels and patches that are completely devoid of channels because of measurement noise (see Roberts et al., 1990). As a result, Eq. 7b may underestimate the number of zero-channel patches expected if few-channel patches are misidentified as having no channels. However, calculations show that the expected number of patches with few channels is insignificant in this model and need not be considered so long as $m \gg 1$.

Clusters of nonzero radius

The assumption that channels are distributed in clusters containing m channels each gives $\langle \eta \rangle = m i_{\text{single}}$. This only applies, however, if channel clusters are so small that a given cluster always falls entirely inside or outside of the patch. If we postulate instead that the characteristic cluster size A_c is significant with respect to patch area A_p, the statistic η will approach i_{single} as A_c/A_p becomes large. In this limit, patches do not sample sufficiently far

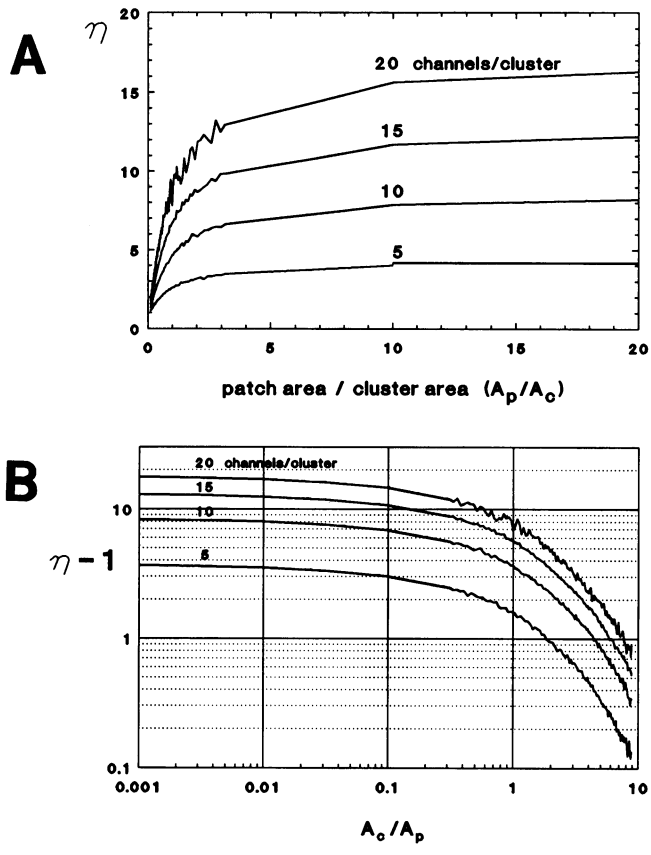

FIGURE 2 Theoretical dependence of η on patch and channel cluster area. (*A*) Monte Carlo analysis of 1,000 patches for m = 5, 10, 15, and 20 channels per cluster. η is plotted in units of channels against patch area in units of cluster area (A_p/A_c). η drops off with small patch areas. (*B*) The same analysis, plotted in coordinates of log ($\eta - 1$) against log cluster area [log (A_c/A_p)]. Half-maximal values are reached when $A_c/A_p = 1$.

from any one channel to detect an increased local density of channels and statistics calculated from them will fail to detect clustering. Therefore, if η is calculated from a data set grouped into bins according to patch area, a drop-off in η for small patch areas might indicate that these patches are smaller than the cluster area.

This prediction is borne out by Monte Carlo simulation of loose patch recording (Fig. 2 *A*). In this simulation, clusters of m channels each are assumed to be distributed randomly in the membrane. Furthermore, the clusters are assumed to be circular with area A_c. η was calculated in units of channels for a range of patch areas A_p, from patches much larger than a cluster (A_c/A_p = 0.001) to very small patches (A_c/A_p = 10). This simulation was done for m = 5, 10, 15, and 20 channels per cluster.

It was found that η equals approximately the value of m for large A_p, until A_p approaches A_c. When $A_c = A_p$, η drops to approximately $m/2$. For patch areas much smaller than the clusters ($A_c/A_p \gg 1$), η falls off asymptotically to 1.

A transformation of this simulation to log-log coordinates reveals a striking resemblance to a Lorentzian function (Fig. 2 *B*). Previous theoretical and experimental work (Anderson and Stevens, 1973) led to an analysis of endplate current noise spectra. These spectra, plotted as a function of frequency, also followed a Lorentzian function; the corner frequency of the function was interpreted by them as reflecting the mean open time of single channels in their system. Our interpretation of the clustering simulations is analogous and is as follows.

Patch experiments will only fully reveal the presence of channel clustering when a patch samples channel clusters in their entirety. If clusters are large with respect to patch area, it is more likely that a given cluster will straddle the boundary of the patch so that parts of clusters are measured rather than all or none. In the limit $A_c \gg A_p$, clustering will go undetected and thus η approaches i_{single}.

This property of η can be turned to advantage if data are available spanning a large range of patch areas A_p. If data are binned by patch area and η calculated for each bin, the clustering model predicts that η will be constant for patch areas greater than $\sim 10A_c$. At $A_p = 10A_c$, the expected value of η is $\sim$10% below the large-patch value. The expected η is $\sim$50% its large-patch value when $A_c = A_p$. So just as the corner frequency of noise spectra is interpreted as the characteristic duration of a channel opening, the turning point of the spectra in Figure 2 *B* gives the characteristic area of a clustering "event."

We emphasize that the simulation does not give a Lorentzian function. The particular form of the curves in Fig. 2 depends on the shape of clusters and patches postulated in the model. Otherwise we would have been able to derive the function analytically, instead of being forced to resort to numerical simulation.

RESULTS

Fig. 3 shows a loose patch data set from a giant neuron in the pedal ganglion of the nudibranch *Doriopsilla.* This data set was generated by recording the I_A current density in 31 patches on a single neuron cell body in voltage clamp experiments. This was done using a loose patch current recording method and four patch electrodes ranging from 4 to 15 μm in tip diameter. Due to membrane infolding (Mirolli and Talbot, 1972; Johnson and Thompson, 1989), each electrode produced patches that were quite variable in area. The average channel density for this data set is 0.26 channel/μm^2 and the average patch area is 113 μm^2, giving an average of 29.3 channels per patch. The single channel current is 0.33 pA.

After correction for measurement uncertainty (see Appendix), the computed statistics for this data set are η = 3.28 pA = 9.95 channels and Z = 3. The hypothesis that channels are distributed at random fails since the expected values under that assumption are $\langle \eta \rangle$ = 1.00 ± 0.26 channel and $\langle Z \rangle$ = 0.00035 ± 0.00035. From this

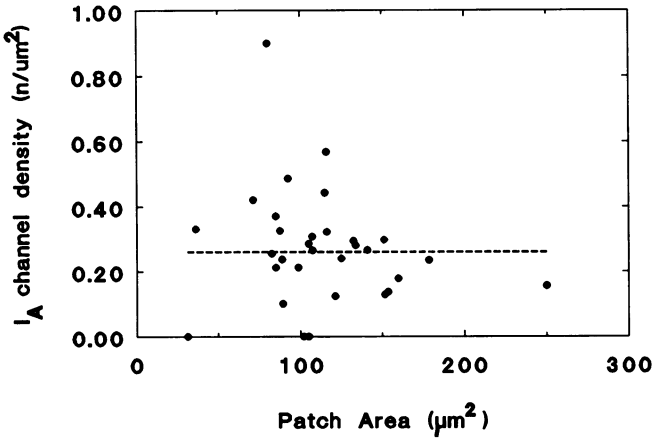

FIGURE 3 Loose patch data from a single molluscan neuron. I_A channel density is plotted against patch area for 31 patches. Data were obtained as described in Premack et al. (1989). The dotted line shows the mean channel density for all patches (0.26 channel/μm^2).

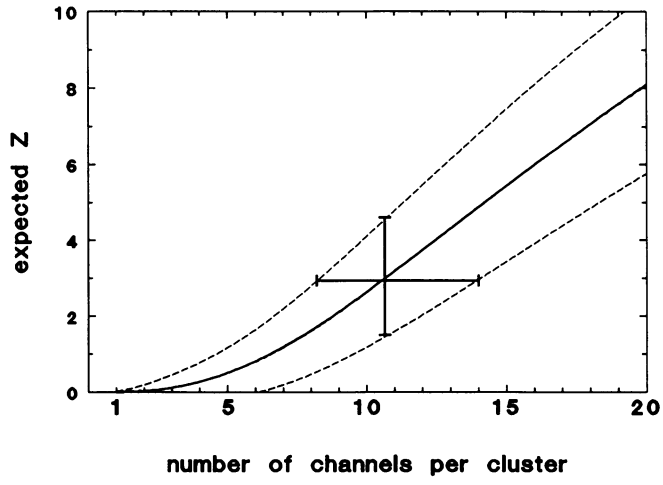

FIGURE 5 Expected mean and variance of Z for a clustered channel distribution. Expected mean of Z was calculated for m = 1–20 channels per cluster, using Eq. 3 and the patch areas and channel density from the molluscan data set of Fig. 3. The dotted lines indicate the envelope of $\pm\sigma$ errors (*vertical bar*), with $\sigma = (\mathrm{Var}(Z))^{1/2}$ as calculated from Eq. 7b. An estimate of m in this model can be made by finding the experimentally determined Z on the solid curve and interpolating a range of values for m (*horizontal error bar*). For Z = 3, m = 10.7 ± 2.9 channels.

we conclude that I_A channels are not randomly distributed over the surface of these molluscan somata.

Model 1, a quiltwork of variable channel densities, can be tested by calculating η as a function of patch area. Fig. 4 shows this calculation for 140 patches drawn from 29 cells. Contrary to the prediction of model 1, η is not proportional to patch area but is relatively constant for patch areas ranging from 31 to 2,750 μm^2. A further test of this model can be made by assuming a simple specific model, a quiltwork of two channel densities. The parameters of this model can be determined by solving Eqs. 6a and 6b for p and q, the fractions of membrane with channel densities d_1 and d_2, respectively. The unique solution for this data set is p = 0.273, d_1 = 0.0010 channel/μm^2, q = 0.727, and d_2 = 0.356 channel/μm^2. With these parameter values, 99.9% of the channels are concentrated in 73% of the surface of the cell, with the remaining 27% of the surface area being nearly devoid of channels (Fig. 1 *B*). Given that zero-channel patches fall nearly exclusively in the low-density zone of this model then, it would be expected that dropping zero-channel patches would reduce the calculated η to 1 since all remaining patches would be sampled from the high density of channels. In fact, excluding zero-channel patches, the calculated value of η is 8.94 channels. These tests show that for these neurons, the observed distribution of I_A channels cannot be explained by models in which channels are randomly distributed with variable density.

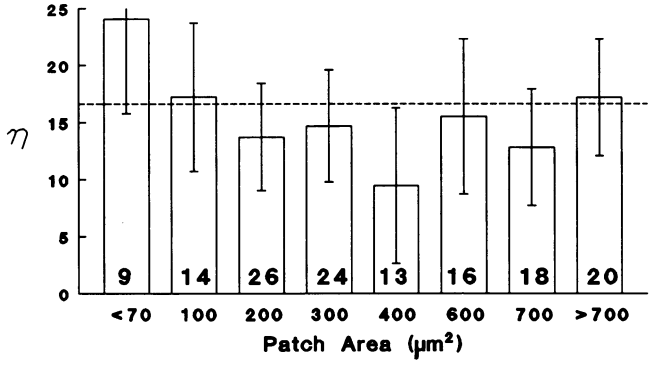

FIGURE 4 Dependence of η on patch area. Area and I_A channel number measurements are from 140 patches on 29 cells. Values of the squared deviation $(x_i - e_i)^2/e_i$ were calculated in units of channels and corrected for measurement error. Horizontal axis labels indicate the maximum patch area used in each bin. Patch areas ranged from 31 to 2,750 μm^2. Error bars were calculated as $(\mathrm{Var}(\eta))^{1/2}$ from Eq. 7a. The horizontal dotted line shows the average η, 16.6. The area dependence expected from the simulation of Fig. 2 *A* does not appear even for the smallest bin of patch areas, indicating a very small cluster area.

The values for η and Z calculated from this data set are consistent with model 2, the Poisson-Poisson clustered model for channel distribution. For this data set, the η statistic predicts $m = \eta - 1 = 9.0 \pm 2.3$ channels per cluster, and the Z statistic predicts that $m = 10.7 \pm 2.9$ channels per cluster. The estimate from Z was made by plotting Z against m for this data set (Fig. 5) and finding the range of m that fell within the error in Z. These analyses give two independent estimates of the number of channels per cluster, and the average of the two is 9.8 ± 1.8 channels per cluster. At the activation voltage used in these experiments, the probability that an individual I_A channel will open during the voltage step is ~0.2. Accordingly, the total number of activatable I_A channels per cluster is 49 ± 9 channels per cluster.

We made an attempt to estimate the spatial dimension of channel clusters. The loose patch data from 29 cells

(2–31 patches per cell, 140 patches) were pooled and grouped by patch area into eight bins (Fig. 4). From the Monte Carlo simulations, we expect a drop-off in the value of n as patch area decreases. The binned data do not exhibit a drop-off as the area of the patch diminishes even for the smallest bin, which corresponds to an average patch area of 49 μm^2. We used the error bars on the bins for $A_p < 100$ μm^2 and the model of Fig. 2 *B* to calculate that $A_c < 3.1$ μm^2 with 90% confidence. Assuming circular channel clusters, this corresponds to a cluster radius of <1.0 μm. This is smaller than the mean distance between randomly distributed clusters (cluster density)$^{-1/2}/2 = 3.2$ μm. The fact that $Z = 3$ also supports the conclusion that cluster size is smaller than intercluster distance, since larger clusters would give a data set with fewer or no zero-channel patches. Computer simulations of Z did not impose a stronger limit on cluster area (data not shown).

The same statistical techniques were applied to the patch-clamp data set provided by Roberts et al. (1990) on the spatial distribution of calcium-dependent K current in bullfrog hair cells. In their analysis, a scatter plot of relative patch current density versus patch area was fit to a maximum likelihood model with an arbitrary measurement noise parameter. If we follow Roberts et al. and omit one patch in which 23% of the whole-cell $I_{K(Ca)}$ was found in 1.4% of the basolateral membrane area, we calculate a value of $\eta = 38.4$ channels for their data set. We use their assumption that $\sigma_I = 0.32$ and Eq. A1 to correct this to a "true" value of 27.9. This is consistent with a Poisson-Poisson model for channel clustering with $m = 26.9 \pm 5.3$ channels per cluster. This value is in good agreement with their conclusion that calcium-dependent K channels are distributed in clusters of ~29 channels each, with ~24 clusters per cell. Note that although the noise estimate is a freely varying parameter of their model rather than a measured variable, our estimate of the number of channels per cluster matches theirs without adjustment of this parameter.

DISCUSSION

A normalized chi-squared statistic for channel number, η, and the number of observed zero-channel patches in a data set, Z, provide good statistical indicators of nonrandom channel distributions in data generated by patch-clamp experiments. By using these statistics on the data of Premack et al. (1989), we conclude that I_A channels are arranged in clusters averaging about 50 channels each, distributed randomly over the surface of the cell. A drop-off in η versus decreasing patch area is not observed, indicating that these clusters are smaller than 2 μm in diameter. A graphical representation of this model is given in Fig. 1 *C*.

The following conditions are sufficient to apply our analysis: (*a*) patches must not overlap each other, to ensure independence of samples; (*b*) no gradients in current density are observed over the surface of the cell; and (*c*) if data are to be pooled from different cells, current density must be known for each individual cell. In the experimental design, electrodes should be as small in area as possible so that variations in current will be large relative to measurement errors; this also maximizes the likelihood of observing zero-channel patches. Using a range of electrode areas will allow a test of variable channel-density models such as model 1 in this paper. A range of electrode areas also allows determination of cluster size; the smallest cluster dimension detectable will be within an order of magnitude of the smallest patch areas obtained. Finally, if single-channel measurements are available, then current clustering can be converted to units of channels to determine how many channels are present in a cluster.

Another prerequisite for this analysis is the accurate determination of patch area and current. These conditions are not always met in gigaseal patch recording, in which membrane-distorting suction is often needed to make the seal. Karpen et al. (1991) observed apparent clustering of cGMP-dependent cation channels in excised patches from salamander retinal rods; this effect disappeared when they switched to a loose-patch recording method. For this reason we regard our analysis as applicable principally to measurements not requiring suction before measurement of patch capacitance. A general treatment of the theoretical effects of measurement errors on the present analysis is given in the Appendix.

We have derived expected values for η and Z for several alternative models of channel distribution. These statistics provide two separate tests to apply to models of nonrandom channel patterning. They are not independent of one another, but in the present analysis we found that the calculated η was the same with or without zero-current patches. A satisfactory model of channel patterning must match predictions for both η and Z. Although more complex models of channel clustering than those presented in this paper are certainly possible, the simplicity of the models presented here allows general conclusions on the nature of channel patterning to be made. One benefit of this approach is that more complex models of channel patterning can in most cases be reducible to one of the two nonrandom models presented here. Note that the present analysis supersedes a less-than-adequate analysis made by us previously (Premack et al., 1989).

If the data set is sufficiently large and spans a range of patch areas, an upper limit on channel cluster dimension can be set by looking for a drop-off in η versus decreasing patch area. This interpretation is analogous to those inferred from spectral noise analysis, with patch area rather than time as the independent variable (Anderson and Stevens, 1973).

Treatment of the data of Roberts et al. using our technique supports the conclusions they have drawn. Their conclusions were based on an iterative computer model

that varied the number of channels per cluster (m) and the measurement uncertainty (σ_I). The compatibility of any given model was assessed by a log-likelihood calculation. In our analysis, a calculation of η and Z can be done using a hand calculator and judicious consideration of experimental techniques. However, our analysis requires an independent measurement of the current measurement uncertainty, σ_I.

Why are A-channels clustered on these molluscan cell bodies? Unlike Ca-dependent K channels, the electrophysiological contribution of A-current to membrane excitability is not expected to be influenced by channel clustering on the scale demonstrated here. It may be that observed channel clustering here reflects packaging of channels and vesicle insertion in the membrane. The clustering we observe would be accounted for if, once inserted, channels were anchored in the membrane to each other or to a cytoskeletal network, as has been observed for sodium channels (Angelides et al., 1988). Accumulation of channels in clusters would reduce the later metabolic energy needed to fabricate channel hotspots. This would be especially useful in the case of sodium channels, which are concentrated in spike-initiating zones. However, we have no evidence yet that the clusters we observe are static or have their origins at the time of channel insertion in the membrane.

APPENDIX

It is necessary to consider the effect of experimental error in the measurement of patch current density on the expected values of η and Var (η). This was done by expressing the uncertainty in observed and expected current, x_i and e_i, as fractions σ_x and σ_e of their measured values. The magnitude of these errors depends on uncertainty in channel number, patch area, and expected channel density. Here we apply standard methods of error propagation to the formulas for η and Var(η) to give the dependence of these expressions on σ_x and σ_e. The result of this analysis is two correction terms. One, η', must be subtracted from η computed from the data set to give a true value, and one, [Var (η)]', must be added to the theoretical Var (η) to give a variance that reflects measurement uncertainty.

In our error analysis, uncertainty in the number of channels in a patch is represented as a fraction σ_x of the current measured in the patch, x. In the A-current data considered here, the main contributor to σ_x is the stochastic nature of channel gating. If the probability of channel opening is p under the conditions in which the patch current density is measured, the number of channels in the patch has fractional uncertainty $\sigma^2 = (1 - p)/x$. To minimize this uncertainty, experiments should be designed to set the probability of channel opening as high as possible. Other contributions to σ_x include noise terms to the recording apparatus, stray capacitance, and the finite resistance of the seal formed between the electrode and the membrane. In the A-current data, these errors are less than ±5% (10% peak-to-peak) (Johnson and Thompson, 1989). A separate source of potential error is the uncertainty in determining the single-channel current amplitude, which must be known to determine the number of active channels in a patch. If each of these error sources is independent of the others, the individual uncertainties may be added in quadrature to give a total σ_x (Bevington, 1969).

The fractional uncertainty in the expected current is similarly represented as σ_e. In this case, uncertainty in current density d_i and patch area A_i both contribute to σ_e. In loose patch recordings, the channel density is calculated by pooling all patches for a single cell and dividing the total number of channels by the total patch area. We were unable to use whole-cell measurements in estimating somatic channel density, owing to the high density of A-current in the axon. Uncertainties in d and A are added in quadrature to give σ_e.

The result of theoretical error analysis using σ_x and σ_e is that experimentally determined values of η are larger than the values of η that would be obtained in an experiment with no channel measurement error ($\sigma_x = 0$). The additional component η', which must be subtracted from the calculated value of η, is

$$\eta' = \sigma_x^2 \bar{x} i_{\text{single}} + \left[\frac{1}{2\sigma_e} \ln\left(\frac{1 + \sigma_e}{1 - \sigma_e}\right) - 1\right](\eta + \bar{x}) i_{\text{single}}. \quad \text{(A1)}$$

The second term was computed for a uniform error distribution for e; it is insignificant if $\sigma_e < 0.1$.

The errors σ_x and σ_e also affect the confidence intervals for each of the individual models of channel patterning. The corrections in this case depend on both σ_x and σ_e and are different for the different models. Correction terms must be added to the theoretical variance Var (η) to arrive at a new confidence interval for the model in question. The correction term [Var (η)]' is

$$[\text{Var}\,(\eta)]' = 4\sigma_x^2\,\text{Var}\,(\eta) + \sigma_e^2\eta^2. \quad \text{(A2)}$$

For the A-current data set, the probability of channel opening was at most 0.2. The resulting uncertainty in channel numbers accounted for over 98% of the correction term η', which was between $0.8i_{\text{single}}$ and $1.2i_{\text{single}}$ for all experiments. For the data of Roberts et al. (1990) on hair cells, we based our corrections on their fit to a model that included uncertainty in current measurements. This uncertainty, which stems from the high minimum uncertainty associated with the method of variance-mean measurements of current, is $\sigma_I = 0.32$, and we assume $\sigma_x = \sigma_I$ for our analysis of their data.

In summary, when Eqs. A1 and A2 are applied to the data sets at hand, we find that the correction η' is significant for both data sets analyzed here: molluscan loose patch and bullfrog hair cell data. The correction [Var (η)]' is not significant, except in experiments in which channel density was not known accurately for individual cells.

Finally, it must be noted that all conclusions drawn from η are in units of observed channels. Clustering parameters can be normalized by a factor equal to the open probability of a channel under the condition of time and voltage at the time the current measurement is taken. This correction requires accurate knowledge of the voltage dependence and kinetics of channel gating derived from voltage clamp experiments.

We thank Brett Premack for suggestions and for the single-channel measurements. Bill Roberts very kindly made available the hair cell data set. An anonymous reviewer made several valuable comments.

This work was supported by NSF grant 9021217 and NIH grant 14519 (to S. Thompson), the Myers Marine Biology Trust, and the Lerner-Gray Fund for Marine Research (to S. Wang).

REFERENCES

Almers, W., and C. Stirling. 1984. Distribution of transport proteins over animal cell membranes. *J. Membr. Biol.* 77:169–186.

Almers, W., R. Fink, and N. Shepherd. 1982. Lateral distribution of ionic channels in the cell membrane of skeletal muscle. *In* Disorders of the Motor Unit. D. L. Schotland, editor. John Wiley and Sons, New York. 349–366.

Anderson, C. R. and C. F. Stevens. 1973. Voltage clamp analysis of acetylcholine produced end-plate current fluctuations at frog neuromuscular junction. *J. Physiol. (Lond.)*. 235:655–691.

Angelides, K. J. 1986. Fluorescently labeled Na channels are localized and immobilized to synapses of innervated muscle fibers. *Nature (Lond.)*. 321:63–66.

Angelides, K. J., L. W. Elmer, D. Loftus, and E. Elson. 1988. Distribution and lateral mobility of voltage-dependent sodium channels in neurons. *J. Cell Biol.* 106:1911–1925.

Beam, K. G., J. H. Caldwell, and J. T. Campbell. 1985. Na channels in skeletal muscle concentrated near the neuromuscular junction. *Nature (Lond.)*. 313:588–590.

Bevington, P. R. 1969. Data Reduction and Error Analysis for the Physical Sciences. McGraw-Hill, New York. 336 pp.

Brehm, P., E. Yeh, J. Patrick, and Y. Kidokoro. 1983. Metabolism of acetylcholine receptors on embryonic amphibian muscle. *J. Neurosci.* 83:751–769.

Catterall, W. 1981. Localization of sodium channels in cultured neural cells. *J. Neurosci.* 1:777–783.

Cramér, H. 1945. Mathematical Methods of Statistics. Princeton University Press, Princeton, New Jersey. 575 pp.

Diggle, P. J. 1983. Statistical Analysis of Spatial Point Patterns. Academic Press, New York. 148 pp.

Ellisman, H. H., and S. R. Levinson. 1982. Immunocytochemical localization of sodium channel distribution in the excitable membranes of Electrophorous electricus. *Proc. Natl. Acad. Sci. USA.* 79:6707–6711.

Johnson, J. W., and S. Thompson. 1989. Measurement of nonuniform current densities and current kinetics in *Aplysia* neurons using a large patch method. *Biophys. J.* 55:299–308.

Karpen, J. W., D. A. Loney, and D. A. Baylor. 1991. Spatial distribution of cyclic GMP-activated channels in salamander retinal rods and variation of density in excised membrane patches. *J. Gen. Physiol.* 98:14a.

Katz, B., and R. Miledi. 1969. Tetrodotoxin-resistant electric activity in presynaptic terminals. *J. Physiol. (Lond.)*. 203:459–487.

Llinas, R., and C. Nicholson. 1971. Electrophysiological properties of dendrites and somata in alligator Purkinje cells. *J. Neurophysiol.* 34:532–551.

Mirolli, M., and S. R. Talbot. 1972. The geometrical factors determining the electrical properties of a molluscan neurone. *J. Physiol. (Lond.)*. 227:19–34.

Pielou, E. C. 1977. Mathematical Ecology. John Wiley & Sons, New York. 385 pp.

Poo, M.-M. 1985. Mobility and localization of proteins in excitable membranes. *Annu. Rev. Neurosci.* 8:369–406.

Premack, B. A., S. Thompson, and J. Coombs-Hahn. 1989. Clustered distribution and variability in kinetics of transient K channels in molluscan neuron cell bodies. *J. Neurosci.* 9:4089–4099.

Roberts, W. M., R. A. Jacobs, and A. J. Hudspeth. 1990. Colocalization of ion channels involved in frequency selectivity and synaptic transmission at presynaptic active zones of hair cells. *J. Neurosci.* 10:3664–3684.

Stuhmer, W., and W. Almers. 1982. Photobleaching through glass micropipettes: sodium channels without lateral mobility in the sarcolemma of frog skeletal muscle. *Proc. Natl. Acad. Sci. USA.* 79:946–950.

Thompson, S., and J. Coombs. 1988. Spatial distribution of Ca currents in molluscan neuron cell bodies and regional differences in the strength of inactivation. *J. Neurosci.* 8:1929–1939.

Young, S. H., and M.-M. Poo. 1983. Topographical rearrangement of ACh receptors alters channel kinetics. *Nature (Lond.)*. 304:161–163.